ENHANCED SEMI-EMPIRICAL FORMULATION FOR (p,n) CROSS SECTIONS AT 12.4 MeV

Lyes Omeir†, Naima Amrani

Physics Department, Setif 1 University, Setif, Algeria

Received 20 December 2025, accepted 30 March 2026, published online 23 June 2026

In this study, we present an improved formulation for calculating (p,n) reaction cross sections at a proton energy of 12.4 MeV. This new approach is based on updated experimental data (EXFOR 2026), a revised compilation of non-elastic cross sections using the TALYS nuclear reaction code, and a re-evaluation of the empirical adjustment parameters. The proposed model builds upon the work of Broeders and Konobeyev (2008) and integrates key theoretical elements of the compound nucleus regime, including the semi-empirical mass formula and the statistical evaporation model. Comparisons with TALYS calculations, which include both statistical and pre-equilibrium contributions, demonstrate the validity of our approach at 12.4 MeV, where compound nucleus mechanisms dominate. The revised six-parameter formulation demonstrates excellent agreement with the latest experimental data and yields significantly reduced values for the statistical deviation metrics Σ and χ^2. This work contributes to the refinement of nuclear reaction models and provides a reliable tool for cross-section prediction in applied and fundamental nuclear science.

DOI:10.5506/APhysPolB.57.7-A4

1. Introduction

Proton-induced nuclear reactions have long been a subject of interest due to their broad applications in fields such as medicine, particle physics, energy production, and fundamental research. Among these, the (p,n) reaction plays a particularly crucial role in the production of radionuclides for medical diagnostics and therapy, as well as in studies of nuclear structure and reaction mechanisms [1].

The increasing need for accurate nuclear data has driven researchers to develop more refined theoretical models and parameterizations. These models, including those based on the exciton and evaporation mechanisms, aim to describe the complex interaction between an incident proton and a target nucleus. Experimental observations are essential to validate and calibrate

† Corresponding author: cherlyes2002@yahoo.fr

these models, especially in cases where direct measurements are limited or unfeasible. Thus, the synergy between experimental data and theoretical modeling forms the cornerstone of reliable nuclear data evaluations [2–5].

In this study, we focus on the (p, n) reaction at an incident proton energy of 12.4 MeV — an energy range of particular importance for applications in nuclear medicine and intermediate-energy physics. Our main objective is to construct a nuclear data library based on this reaction, combining theoretical modeling and updated experimental compilations. By doing so, we aim to enhance the predictive capability of existing nuclear reaction models and extend their applicability to isotopes or conditions beyond the reach of experimental investigation.

The methodology involves several key steps: the collection and critical evaluation of available experimental data for (p, n) reactions at 12.4 MeV, followed by the development and adjustment of theoretical models to fit this data accurately. Finally, we propose an improved semi-empirical formula, rooted in the framework of the statistical evaporation model, and semi-empirical mass systematics.

More specifically, we present a revised six-parameter formulation derived from the work of Konobeyev *et al.* [6], which offers significantly better agreement with the experimental cross sections for a broad range of isotopes. The ultimate goal of this work is to provide the nuclear science community with a reliable, accurate, and accessible (p, n) cross-section dataset at 12.4 MeV, contributing both to theoretical insight and practical applications in the field.

2. Materials and methods

In this section, we first address the TALYS code, an advanced computational tool widely used for the modeling and prediction of nuclear data. We briefly present its operating principles, fields of application, and the essential parameters employed in our simulations. In the second part, we describe the nuclei investigated in this work, specifying their physical characteristics and their relevance in the context of cross-section calculations, there by establishing a clear connection between the simulation tool and the nuclear systems under analysis.

2.1. TALYS code and non-elastic cross sections

TALYS is a comprehensive nuclear reaction modeling tool designed to simulate reactions induced by neutrons, photons, protons, deuterons, tritons, ^{3}He, and alpha particles across a broad energy range (from eV to 200 MeV), for target nuclei with $A \geq 12$ [7]. It incorporates multiple theoretical models within a unified framework, including optical models, compound nucleus formation, pre-equilibrium emission, and fission dynamics.

In this study, TALYS is used primarily to calculate non-elastic cross sections and to evaluate the pre-equilibrium contribution to particle emission.

As illustrated in Fig. 1, the non-elastic cross sections of all isotopes involved in this study have been calculated at 12.4 MeV using the TALYS nuclear code.

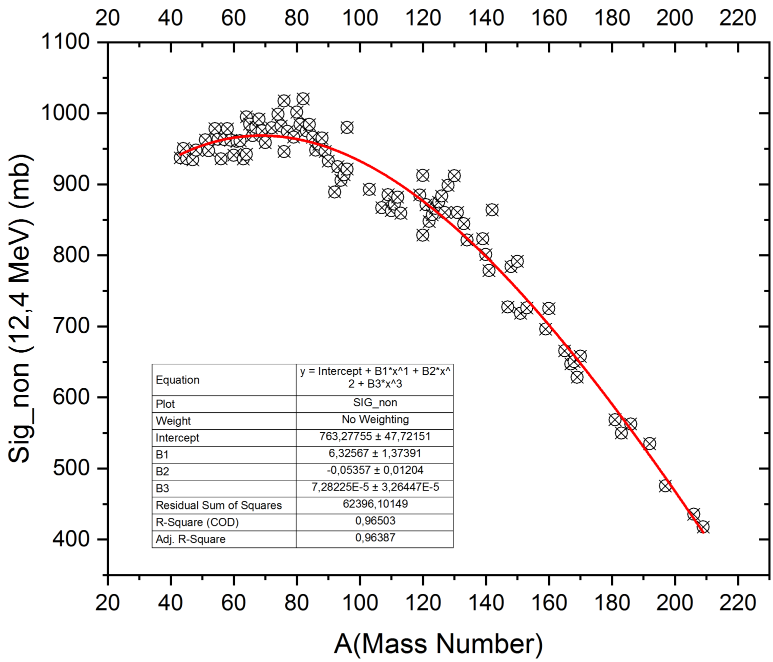

Fig. 1. Non-elastic cross sections calculated by TALYS code for stable nuclei with $43 \le A \le 209$ at 12.4 MeV.

These $\sigma_{\rm non}(12.4\ {\rm MeV})$ values are approximated by

$$\sigma_{\rm non}(12.4\ {\rm MeV}) = 763.277 + 6.325A - 0.05357A^2 + 7.282 \times 10^{-5}A^3\,. \quad (1)$$

2.2. Analysis of (p, n) reactions based on energy thresholds

It is convenient to classify target nuclei into two categories based on the threshold of the $(p, 2n)$ reaction relative to the incident energy of 12.4 MeV. This classification is justified because the emission of a second neutron becomes energetically feasible only when the $(p, 2n)$ threshold is lower than the incident proton energy.

2.2.1. Nuclei with $(p, 2n)$ reaction thresholds above 12.4 MeV

At the incident energy of 12.4 MeV considered in this study, (p, n) reactions proceed predominantly via compound nucleus formation followed by statistical evaporation. This energy falls within the optimal validity domain of the Hauser–Feshbach model (8–25 MeV), where statistical mechanisms largely prevail over direct and pre-equilibrium processes. Among the isotopes studied, 31 nuclei present $(p, 2n)$ reaction thresholds above 12.4 MeV. For these nuclei, the (p, n) reaction occurs through compound nucleus formation followed by statistical evaporation, with fewer competing pathways than for nuclei where the $(p, 2n)$ reaction is energetically allowed. This configuration simplifies the analysis by reducing the number of competing decay channels. The derivation presented here builds upon the Hauser–Feshbach model [8], as previously detailed in our prior work [9], but briefly summarized below for completeness.

The non-elastic reaction cross section σ_{non} at 12.4 MeV and the decay widths Γ_n (neutrons) and Γ_p (protons) determine the (p, n) cross section

$$\sigma_{(p,n)} = \sigma_{\mathrm{non}}(12.4\ \mathrm{MeV})\frac{\Gamma_n}{\Gamma_n + \Gamma_p}\,. \tag{2}$$

The decay widths are calculated as follows:

$$\Gamma_p = \frac{(2J_p+1)M_p}{\pi\hbar^2}R^2T_p^2\left(1-\frac{U_p}{\varepsilon_p}\right)\exp\left(-\frac{U_p+B_p+\delta_p}{T_p}\right), \tag{3}$$

$$\Gamma_n = \frac{(2J_n+1)M_n}{\pi\hbar^2}R^2T_n^2\exp\left(-\frac{B_n+\delta_n}{T_n}\right), \tag{4}$$

where M_p, J_p, U_p, ε_p, B_p, and δ_p denote, respectively, the mass, spin, Coulomb barrier, emitted energy, separation energy, and shell correction of the proton. Analogous parameters are defined for neutrons.

The Q-value of the reaction is expressed as

$$Q_{(p,n)} = U_p + B_p + \delta_p - B_n - \delta_n\,. \tag{5}$$

A semi-empirical approximation of this Q-value is given by

$$Q_{(p,n)} = \alpha_1\left(\frac{N-Z-1}{A}\right) + \alpha_2\frac{Z}{A^{1/3}}\,, \tag{6}$$

with α_i representing empirical constants. The nuclear temperatures are given by

$$T_p^2 \approx \frac{C\theta E_p}{A}\,, \tag{7}$$

$$T_n^2 \approx \frac{C\left(\theta E_p + Q_{(p,n)}\right)}{A}\,, \tag{8}$$

where $\theta = A/(A+1)$ and C is a constant linked to the level density parameter. Substituting this into the cross section formula, one obtains

$$\sigma_{(p,n)} = \frac{\sigma_{\mathrm{non}}(12.4\ \mathrm{MeV})}{1+\exp\left[\sqrt{\frac{A}{4C\theta E_p}}\left(\frac{Q^2_{(p,n)}}{\theta E_p} - Q_{(p,n)} - 2U_p\right)\right]} \,. \tag{9}$$

This motivates the following six-parameter empirical formula:

$$\sigma_{(p,n)} = \frac{\sigma_{\mathrm{non}}(12.4\ \mathrm{MeV})}{\exp\left[A^{\lambda_1}(\lambda_2 S^2 + \lambda_3 S + \lambda_4 \Phi + \lambda_5) + \lambda_6\right]} \,, \tag{10}$$

where

— $S = (N - Z - 1)/A$ (asymmetry parameter);
— $\Phi = Z/A^{1/3}$ (Coulomb term);
— λ_i are fitting parameters.

2.2.2. Nuclei with $(p, 2n)$ reaction thresholds below 12.4 MeV

For nuclei in which the $(p, 2n)$ reaction threshold lies below 12.4 MeV, the probability of a second neutron emission becomes non-negligible and must be considered in the analytical modeling of the (p, n) cross section. In this case, part of the reaction flux is shared with the $(p, 2n)$ channel, leading to a reduction in the observable (p, n) yield. Following the approach of Broeders *et al.* [3], the cross section can be written as

$$\sigma_{(p,n)} = \sigma_{\mathrm{non}} \frac{\Gamma'_n}{\Gamma_n + \Gamma_p} = \frac{\Gamma'_n/\Gamma_n}{1 + \Gamma_p/\Gamma_n} \,, \tag{11}$$

where Γ_n and Γ_p are the total neutron and proton decay widths, and Γ'_n represents the partial neutron width in the energy interval from $\theta E_p + Q_{(p,2n)}$ to $\theta E_p + Q_{(p,n)}$, with $\theta = A/(A+1)$. Integrating over this interval, one obtains an approximation for the partial width ratio

$$\frac{\Gamma'_n}{\Gamma_n} = \exp\left[-\frac{\theta E_p + Q_{(p,2n)}}{T_n}\right]\left(1 + \frac{\theta E_p + Q_{(p,n)}}{T_n}\right) . \tag{12}$$

The Q-value for the $(p, 2n)$ reaction is approximated using a semi-empirical expansion

$$Q_{(p,2n)} = \alpha_1\left(\frac{N-Z-3}{A}\right)^2 + \alpha_2\left(\frac{N-Z-1.5}{A}\right) + \alpha_3\frac{(Z+1)^2}{A^{4/3}} + \alpha_4\frac{Z}{A^{1/3}} + \alpha_5\frac{1}{A^{1/3}} + \alpha_6 \,, \tag{13}$$

where N, Z, and A are the neutron, proton, and mass numbers of the target nucleus, and α_i are fit parameters. Using the results of Eqs. (11), (12), and (13), a six-parameter semi-empirical formula is proposed for the (p,n) cross section in this case

$$\begin{aligned}\sigma_{(p,n)} &= \sigma_{\text{non}}(12.4\ \text{MeV})\exp\left[A^{1/2}\left(\gamma_1 K^2 + \gamma_2 W + \gamma_3 V + \gamma_4\right)\right] \\ &\quad + \left(1 + A^{1/2}\left(\gamma_5 K^2 + \gamma_6 W\right)\right), \end{aligned} \tag{14}$$

with

— $K = (N - Z - 3)/A$;

— $W = (N - Z - 1.5)/A$;

— $V = Z/A^{1/3}$;

— γ_i: empirical fit parameters.

3. Results

3.1. Nuclear excitation functions for (p,n) processes

In this study, the reaction threshold energies were determined for each isotope using the QCALC tool provided by the Nuclear Data Services of Brookhaven National Laboratory[1]. For endothermic reactions, the threshold energy E_{th} is calculated using the expression

$$E_{\text{th}} = \frac{m_3 + m_4}{m_3 + m_4 - m_1}\,|Q|\,, \tag{15}$$

where m_1 and m_3 denote the masses of the incident and outgoing particles, respectively, and m_4 is the mass of the residual nucleus. Q is the reaction Q-value derived from mass differences [10].

Experimental excitation functions for (p,n) reactions were collected for 95 stable target nuclei with mass numbers $43 \leq A \leq 209$. Among these, 31 nuclei exhibit $(p,2n)$ reaction thresholds greater than 12.4 MeV. The data were extracted from the EXFOR2026 database in the energy interval 12.0–12.8 MeV. Where necessary, the cross sections were interpolated or extrapolated to 12.4 MeV using suitable statistical software.

To obtain a representative value at 12.4 MeV, each dataset was statistically analyzed using the weighted average method as follows [6]:

$$\langle\sigma^{\exp}\rangle = \frac{\sum_{j=1}^{n}\sigma_j/(\Delta\sigma_j)^2}{\sum_{j=1}^{n}1/(\Delta\sigma_j)^2}\,, \tag{16}$$

$$\langle\Delta\sigma^{\exp}\rangle = \max(\Delta\sigma_A, \Delta\sigma_B)\,, \tag{17}$$

[1] http://www.nndc.bnl.gov/qcalc/

with the statistical uncertainties defined as

$$\Delta\sigma_A = \sqrt{\frac{\sum_{j=1}^{n}(\sigma_j - \langle\sigma^{\exp}\rangle)^2/(\Delta\sigma_j)^2}{(n-1)\sum_{j=1}^{n}1/(\Delta\sigma_j)^2}}\,, \tag{18}$$

$$\Delta\sigma_B = \left(\sum_{j=1}^{n}\frac{1}{(\Delta\sigma_j)^2}\right)^{-1/2}. \tag{19}$$

Here, σ_j and $\Delta\sigma_j$ represent the experimental cross section and its uncertainty from the j^{th} measurement, while n denotes the number of available experimental data points for a given nucleus. The final evaluated cross section at 12.4 MeV, expressed as $\langle\sigma^{\exp}\rangle \pm \langle\Delta\sigma^{\exp}\rangle$, is summarized for all 95 nuclei in Table 1.

Table 1. Experimental and calculated (p,n) reaction cross sections at 12.4 MeV for 95 target nuclei. The table includes the measured values $\sigma_{\exp} \pm \Delta\sigma_{\exp}$, the calculated cross sections σ_{sys} from Eq. (10) and Eq. (14), and the deviation factor $\sum = \sum_{i=1}^{N}\left(\frac{\sigma_i^{\exp}-\sigma_i^{\text{cal}}}{\Delta\sigma_i^{\exp}}\right)^2$.

Z	A	$\sigma_{\exp} \pm \Delta\sigma_{\exp}$	σ_{sys}	$\sum$	Experimental references
20	43	259.1 ± 17.8	207.8	8.30	[4, 11]
20	44	744.4 ± 35.5	599.9	16.57	[4, 11]
21	45	348.0 ± 27.2	230.5	18.66	[4, 12–15]
22	47	309.2 ± 44.8	261.3	1.14	[4, 16]
22	48	509.6 ± 14.5	461.7	10.90	[4, 16–18]
23	51	430.8 ± 71.8	852.5	34.50	[4, 16, 19–23]
24	52	476.4 ± 26.5	353.4	21.54	[4, 16]
24	54	879.3 ± 87.9	1017.9	2.49	[4]
25	55	444.0 ± 80.0	624.7	5.09	[24]
26	56	390.6 ± 19.5	309.1	17.47	[4, 16, 25, 26]
26	57	348.7 ± 54.5	570.6	16.57	[4, 16, 27]
26	58	718.0 ± 40.1	773.7	1.93	[4, 28, 29]
27	59	604.3 ± 60.4	478.7	4.32	[23]
28	60	302.3 ± 16.0	301.6	0.00	[4, 14, 30–33]
28	61	383.9 ± 27.7	487.0	13.86	[14, 16, 30, 33, 34]
28	62	619.2 ± 130.9	630.5	0.00	[4, 33, 35]
28	64	571.6 ± 78.5	772.9	6.58	[4, 14, 16, 31, 33, 34, 36, 37]

Continuation of Table 1

Z	A	$\sigma_{\rm exp} \pm \Delta\sigma_{\rm exp}$	$\sigma_{\rm sys}$	$\sum$	Experimental references
29	63	424.5 ± 14.6	448.3	2.66	[4, 38–41]
29	65	686.2 ± 16.9	667.3	1.24	[4, 39, 42–44]
30	64	369.0 ± 44.0	311.0	1.74	[45]
30	66	612.1 ± 20.9	598.0	0.45	[4, 14, 40, 46–49]
30	67	573.9 ± 53.1	641.4	1.61	[4, 47–50]
30	68	776.8 ± 25.1	658.1	22.36	[4, 12, 14, 40, 47, 48, 50–52]
31	69	851.8 ± 66.1	563.3	19.05	[4, 14, 53]
32	70	603.7 ± 60.4	540.5	1.09	[4]
32	72	914.6 ± 91.5	643.8	8.75	[4]
32	74	924.9 ± 92.5	534.9	17.77	[4]
32	76	365.6 ± 36.6	395.0	0.65	[4]
33	75	607.1 ± 115.1	545.1	0.29	[4, 54, 55]
34	76	614.1 ± 94.6	638.9	0.06	[4, 56, 57]
34	77	608.7 ± 160.9	643.5	0.04	[4, 56]
34	80	741.0 ± 53.0	381.9	45.89	[4]
34	82	340.1 ± 34.0	249.7	7.06	[4]
35	79	663.9 ± 65.2	501.7	6.18	[4, 58, 59]
35	81	401.0 ± 16.0	436.5	4.93	[58]
36	83	658.0 ± 95.0	640.9	0.03	[60]
36	84	500.4 ± 75.1	375.7	2.75	[60]
37	85	717.4 ± 115.8	425.0	6.37	[4, 61]
38	86	718.4 ± 152.4	637.0	0.28	[4, 62, 63]
38	87	767.9 ± 268.7	637.5	0.23	[4, 62]
38	88	954.8 ± 63.5	636.8	25.08	[4, 62, 64]
39	89	724.9 ± 20.4	635.3	19.28	[14, 65–70]
40	90	865.6 ± 73.2	628.6	10.48	[4, 71]
40	96	103.5 ± 10.4	183.0	58.24	[4]
41	93	631.2 ± 63.1	425.1	10.67	[23]
42	92	420.3 ± 59.5	510.8	2.31	[72]
42	94	641.5 ± 37.4	613.2	0.57	[4, 63, 72]
42	95	789.2 ± 113.6	624.4	2.10	[4, 72]
42	96	834.0 ± 77.0	394.1	32.63	[4, 72]
45	103	325.3 ± 40.5	383.7	18.92	[73, 74]

Continuation of Table 1

Z	A	$\sigma_{\text{exp}} \pm \Delta\sigma_{\text{exp}}$	σ_{sys}	$\sum$	Experimental references
47	107	496.0 ± 34.0	416.0	5.53	[39]
47	109	261.0 ± 31.0	319.3	3.55	[75]
48	110	824.2 ± 62.5	600.5	12.80	[76, 77]
48	111	792.8 ± 40.9	338.6	123.32	[14, 76–78]
48	112	638.0 ± 138.2	287.7	6.42	[76, 77]
49	113	655.0 ± 69.0	359.3	18.28	[79]
50	119	998.0 ± 67.0	186.4	146.72	[80]
50	120	438.0 ± 38.0	151.6	56.78	[81]
51	121	439.5 ± 96.6	204.3	5.92	[30, 82]
52	120	513.0 ± 94.0	578.7	0.47	[83]
52	122	537.0 ± 107.4	575.5	0.12	[83]
52	123	648.7 ± 42.7	234.4	98.72	[84, 85]
52	124	353.5 ± 115.1	181.2	2.34	[86, 87]
52	125	466.0 ± 75.0	144.1	18.42	[88]
52	126	320.9 ± 73.1	112.9	8.10	[89]
52	128	123.0 ± 11.5	66.5	24.13	[90, 91]
52	130	92.0 ± 10.0	37.27	29.94	[85]
53	127	227.4 ± 31.2	160.5	4.60	[58, 92]
54	131	505.0 ± 57.0	111.0	47.77	[93]
55	133	325.0 ± 24.0	125.4	69.14	[94]
56	134	118.7 ± 14.2	179.1	18.12	[90]
57	139	180.4 ± 20.4	97.9	16.30	[95]
58	140	947.0 ± 169.0	143.6	22.60	[96]
58	142	122.9 ± 11.5	92.2	7.09	[14, 96, 97]
59	141	554.5 ± 45.4	205.9	58.94	[98, 99]
60	148	53.3 ± 10.7	68.0	1.90	[100]
60	150	19.6 ± 1.5	38.8	174.52	[101]
62	147	392.3 ± 19.0	301.5	22.82	[102]
63	151	119.9 ± 30.0	222.7	11.79	[103]
63	153	180.4 ± 20.4	138.7	4.18	[103]
64	160	43.3 ± 4.7	43.2	0.00	[104, 105]
65	159	98.7 ± 9.2	114.3	2.88	[95, 106]
67	165	95.4 ± 8.6	94.9	0.00	[107–110]

Continuation of Table 1

Z	A	$\sigma_{\text{exp}} \pm \Delta\sigma_{\text{exp}}$	σ_{sys}	$\sum$	Experimental references
68	167	287.0 ± 31.8	112.4	30.14	[111, 112]
68	168	107.4 ± 4.6	86.7	20.08	[111, 112]
68	170	59.1 ± 12.4	50.6	0.46	[112, 113]
69	169	138.2 ± 15.1	133.1	0.11	[114, 115]
73	181	61.1 ± 12.0	97.9	9.45	[116]
74	183	104.4 ± 11.5	181.0	1.39	[117, 118]
74	186	15.6 ± 9.6	53.8	15.84	[117–120]
76	192	47.9 ± 3.2	47.0	0.08	[121]
78	198	50.0 ± 10.0	41.6	0.71	[122]
79	197	80.4 ± 9.9	122.4	10.48	[123–127]
82	206	244.2 ± 36.6	96.8	16.20	[128]
83	209	86.2 ± 8.9	91.6	0.27	[129]

Table 1 summarizes the experimental (p, n) cross sections at 12.4 MeV for 95 nuclei, alongside systematic predictions and corresponding deviation factors.

The comparison between experimental and theoretical (p, n) reaction cross sections is presented in Fig. 2, showing the correlation with the neutron excess parameter $(N - Z)/A$ for nuclei with $43 \leq \text{A} \leq 209$ at 12.4 MeV incident proton energy.

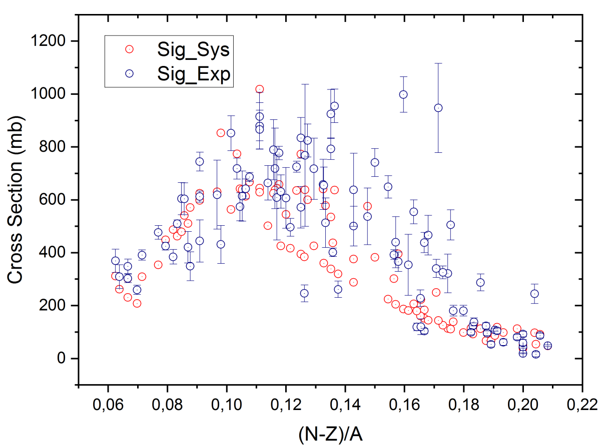

Fig. 2. The (p, n) reaction cross section for nuclei of mass number $43 \leq A \leq 209$ at the incident proton energy of 12.4 MeV obtained from the analysis of experimental data in Table 1 and calculated using systematics, Eqs. (10) and (14), as a function of the parameter $(N - Z)/A$.

3.2. Statistical parameters and quality of fit

To assess the quality of the proposed systematic formulations for (p,n) cross sections at 12.4 MeV, we evaluated two key statistical metrics: the residual sum Σ and the reduced chi-square χ^2. These metrics measure the deviation between calculated and experimental values, and are defined as follows:

$$\Sigma = \sum_{i=1}^{N} \left(\frac{\sigma_i^{\exp} - \sigma_i^{\mathrm{cal}}}{\Delta\sigma_i^{\exp}} \right)^2 , \tag{20}$$

$$\chi^2 = \frac{\Sigma}{N - M} , \tag{21}$$

where N is the number of experimental data points, M is the number of free parameters in the model, $\sigma_i^{\exp}$ and $\Delta\sigma_i^{\exp}$ are the experimental values and their uncertainties, and σ_i^{cal} is the calculated value from the model.

Two parameterizations were tested using 95 experimental datasets from the EXFOR 2026 database.

Table 2. Fitted parameters λ_i for the first proposed six-parameter formulation Eq. (10).

Model	Σ	χ^2	λ_1	λ_2	λ_3	λ_4	λ_5	λ_6
This work	215.3	8.61	-2.3	-5.0711×10^7	4.836×10^6	1.905×10^2	-1.10×10^5	1.5

As presented in Table 2, this first formulation, derived from Eq. (10), exhibits excellent agreement with the experimental excitation functions, achieving the lowest $\Sigma = 215.3$ and reduced $\chi^2 = 8.61$ across the dataset.

Table 3. Fitted parameters γ_i for the alternative six-parameter formulation Eq. (14).

Model	Σ	χ^2	γ_1	γ_2	γ_3	γ_4	γ_5	γ_6
This work	1425.95	24.58	-10.266	0.24499	0.15406	-3.349	1.39×10^9	1.63×10^7

As reported in Table 3, this second formulation, while based on the same theoretical foundations — namely the semi-empirical mass formula and the statistical evaporation model — yields higher deviations from experimental data.

4. Discussion

The analysis of the studied isotopes revealed the necessity of adopting a differential approach based on the energetic availability of reaction channels. The 31 nuclei exhibiting $(p, 2n)$ reaction thresholds above 12.4 MeV constitute a first group, while the remaining nuclei, for which the $(p, 2n)$ channel is energetically accessible, form a distinct second group.

This physically motivated stratification led to the development of two specialized systematic formulations. For the first group (thresholds $(p, 2n) >$ 12.4 MeV), the optimized formulation presents a remarkably low reduced chi-square of $\chi^2 = 8.61$, reflecting the simplified competition between exit channels. This exceptional performance is explained by the fact that the absence of the $(p, 2n)$ channel significantly reduces the complexity of the statistical evaporation process, allowing for more precise predictions of (p, n) cross sections (Table 2).

For the second group (thresholds $(p, 2n) \leq 12.4$ MeV), the adapted formulation achieves $\chi^2 = 24.58$. This higher value, while remaining within an acceptable range for practical applications, reflects the increased complexity of competition between (p, n) and $(p, 2n)$ channels. The simultaneous presence of these two evaporation pathways introduces additional variability that makes systematic prediction more challenging (Table 3).

This performance difference between the two groups validates our theoretical hypothesis that closure of the $(p, 2n)$ channel considerably improves the model's predictive accuracy.

5. Conclusion and outlook

The first systematic formulation, developed for the 31 nuclei with $(p, 2n)$ thresholds above 12.4 MeV, achieves exceptional accuracy with a reduced chi-square value of $\chi^2 = 8.61$ (Table 2). This superior performance reflects the simplified channel competition, where the $(p, 2n)$ pathway is energetically forbidden, allowing the Hauser–Feshbach statistical model to provide highly reliable predictions. The second formulation, tailored for nuclei where the $(p, 2n)$ channel remains energetically accessible, yields $\chi^2 = 24.58$ (Table 3). While higher than the first group, this value remains acceptable for practical nuclear applications, considering the increased complexity of competing evaporation channels at 12.4 MeV. This dual-systematic approach demonstrates that physically motivated stratification of nuclear data significantly improves predictive accuracy. The methodology provides valuable tools for rapid cross-section estimation in medical isotope production, activation studies, and nuclear data library applications, where computational efficiency is prioritized while maintaining acceptable precision. The established framework validates the importance of considering channel availability in systematic development and offers a robust foundation for extending similar approaches to other reaction types and energy ranges.

The authors would like to thank the Nuclear Data Section of the IAEA for providing access to the EXFOR database, and the developers of the TALYS nuclear reaction code for making their software openly available. The authors also acknowledge the support and constructive discussions with colleagues from the Nuclear Physics Department at UFAS 1. No funding was received for this research.

REFERENCES

[1] S.K. Ali *et al.*, «Evaluation of production cross-sections for theranostic ^{67}Cu radionuclide via proton-induced nuclear reaction on ^{68}Zn target», *Appl. Radiat. Isot.* **173**, 109735 (2021).

[2] C.H. Broeders *et al.*, «Proton Activation Data File to Study Activation and Transmutation of Materials Irradiated with Protons at Energies up to 150 MeV», *J. Nucl. Sci. Technol.* **44**, 933 (2007).

[3] C. Broeders, A.Y. Konobeyev, «Systematics of (p,α) $(p,n\alpha)$, and (p,np) reaction cross-sections», *Appl. Radiat. Isot.* **65**, 1249 (2007).

[4] V. Levkovskij, «Activation cross section nuclides of average masses ($A = 40$–100) by protons and alpha-particles with average energies ($E = 10$–50 MeV)», *INTER-VESTI*, Moscow, Russia 1991; https://www-nds.iaea.org/CRP-CP-monitor/2RCM/Hussain-2RCM-2014.pdf

[5] V. Weisskopf, D. Ewing, «On the Yield of Nuclear Reactions with Heavy Elements», *Phys. Rev.* **57**, 472 (1940); *Erratum ibid.* **57**, 935 (1940).

[6] C. Broeders, A.Y. Konobeyev, «Systematics of (p,n) reaction cross-section», *Radiochim. Acta* **96**, 387 (2008).

[7] A. Koning, S. Hilaire, S. Goriely, «TALYS 1.95 nuclear research and consultancy group (NRG)», The Netherlands, 2019.

[8] W. Hauser, H. Feshbach, «The Inelastic Scattering of Neutrons», *Phys. Rev.* **87**, 366 (1952).

[9] O. Lyes, N. Amrani, «New semi-empirical systematic of (p,n) reaction cross section at 7.5 MeV», *Kerntechnik* **88**, 279 (2023).

[10] D.L. Aldama, «Nuclear data services», https://www-nds.iaea.org/publications/iaea-nds/iaea-nds-0210.pdf

[11] T.S. Carzaniga *et al.*, «Measurement of ^{43}Sc and ^{44}Sc production cross-section with an 18 MeV medical PET cyclotron», *Appl. Radiat. Isot.* **129**, 96 (2017).

[12] T. McGee, C. Rao, G. Saha, L. Yaffe, «Nuclear interactions of ^{45}Sc and ^{68}Zn with protons of medium energy», *Nucl. Phys. A* **150**, 11 (1970).

[13] F. Ditrói *et al.*, «Production of ^{45}Ti radioisotope by proton irradiation of natural scandium», *Radiat. Phys. Chem.* **218**, 111572 (2024).

[14] H. Blosser, T. Handley, «Survey of (p, n) Reactions at 12 Mev», *Phys. Rev.* **100**, 1340 (1955).

[15] R.G. Thomas Jr., W. Bartolini, «Excitation functions for (p, n) and $(p, 2n)$ interactions in Sc, Cr, Mo, Cd and W between 8 and 14 MeV», *Nucl. Phys. A* **106**, 323 (1967).

[16] S. Tanaka, M. Furukawa, «Excitation Functions for (p, n) Reactions with Titanium, Vanadium, Chromium, Iron and Nickel up to $Ep = 14$ MeV», *J. Phys. Soc. Jpn.* **14**, 1269 (1959).

[17] E. Gadioli, E. Gadioli Erba, J. Hogan, K. Burns, «Emission of alpha particles in the interaction of 10–85 MeV protons with ^{48,50}Ti», *Z. Phys. A* **301**, 289 (1981).

[18] H. West, R. Lanier, M. Mustafa, «Excitation functions for the nuclear reactions on titanium leading to the production of ^{48}V, ^{44}Sc, and ^{47}Sc, by proton, deuteron and triton irradiations at 0–35 MeV», in: H.I. West Jr. (Ed.) «Some Light-Ion Excitation-Function Measurements on Titanium, Yttrium, and Europium, and Associated Results», *Lawrence Livemore National Laboratory*, 1993.

[19] A. Solieman, M. Al-Abyad, F. Ditroi, Z. Saleh, «Experimental and theoretical study for the production of ^{51}Cr using p, d, ^{3}He and ^{4}He projectiles on V, Ti and Cr targets», *Nucl. Instrum. Methods Phys. Res. B* **366**, 19 (2016).

[20] R. Michel, G. Brinkmann, «On the depth-dependent production of radionuclides $(44 \leq A \leq 59)$ by solar protons in extraterrestrial matter», *J. Radioanal. Chem.* **59**, 467 (1980).

[21] Z. Wenrong, L. Hanlin, Y. Weixiang, «Excitation function of ^{51}V (p, n) ^{51}Cr up to 22 MeV», *Chin. J. Nucl. Phys.* **16**, 67 (1994).

[22] M. Musthafa, M.K. Sharma, B. Singh, R. Prasad, «Measurement and analysis of cross sections for (p, n) reactions in ^{51}V and ^{113}In», *Appl. Radiat. Isot.* **62**, 419 (2005).

[23] G. Chodil *et al.*, «(p, n) and $(p, 2n)$ cross sections of nine elements between 7.0 and 15.0 MeV», *Nucl. Phys. A* **93**, 648 (1967).

[24] M. Al-Abyad, I. Spahn, S. Qaim, «Experimental studies and nuclear model calculations on proton induced reactions on manganese up to 45 MeV with reference to production of ^{55}Fe, ^{54}Mn and ^{51}Cr», *Appl. Radiat. Isot.* **68**, 2393 (2010).

[25] W. Zhao, H. Lu, W. Yu, «Investigation of ^{89}Y (p, n) ^{89}Zr, ^{89}Y $(p, 2n)$ ^{88}Zr and ^{89}Y (p, pn) ^{88}Y reactions up to 22 MeV», *Chin. J. Nucl. Phys.* **14**, 7 (1993).

[26] I. Jenkins, A. Wain, «Excitation functions for the bombardment of ^{56}Fe with protons», *J. Inorg. Nucl. Chem.* **32**, 1419 (1970).

[27] M. Al-Abyad, M. Comsan, S. Qaim, «Excitation functions of proton-induced reactions on $^{\mathrm{nat}}$Fe and enriched ^{57}Fe with particular reference to the production of ^{57}Co», *Appl. Radiat. Isot.* **67**, 122 (2009).

[28] S. Sudár, S. Qaim, «Excitation functions of ^{58}Fe$(p,n)^{58}$Co proton and deuteron induced reactions on iron and alpha-particle induced reactions on manganese in the energy region up to 25 MeV», *Phys. Rev. C* **50**, 2408 (1994).

[29] R. Ghosh *et al.*, «Measurement of reaction cross-section within the proton energy range of 3.38 to 19.63 MeV», *Nucl. Phys. A* **964**, 86 (2017).

[30] B. Singh *et al.*, «A study of pre-equilibrium emission in some proton- and alpha-induced reactions», *Nucl. Instrum. Methods Phys. Res. A* **562**, 717 (2006).

[31] M. Uddin *et al.*, «Excitation function of the ^{60}Ni$(p,\gamma)^{61}$Cu reaction from threshold to 16 MeV», *Phys. Rev. C* **93**, 044606 (2016).

[32] B. Lawriniang *et al.*, «Measurements of ^{60}Ni$(p,n)^{60}$Cu reaction cross-sections and covariance analysis of the uncertainty», *J. Radioanal. Nucl. Chem.* **319**, 695 (2019).

[33] S. Tanaka, M. Furukawa, M. Chiba, «Nuclear reactions of nickel with protons up to 56 MeV», *J. Radioanal. Nucl. Chem.* **34**, 2419 (1972).

[34] F. Szelecsényi, G. Blessing, S. Qaim, «Excitation functions of proton induced nuclear reactions on enriched ^{61}Ni and ^{64}Ni: Possibility of production of no-carrier-added ^{61}Cu and ^{64}Cu at a small cyclotron», *Appl. Radiat. Isot.* **44**, 575 (1993).

[35] H. Piel, S. Qaim, G. Stöcklin, «Excitation Functions of (p,xn)-Reactions on Ni and Highly Enriched Ni: Possibility of Production of Medically Important Radioisotope ^{62}Cu at a Small Cyclotron», *Radiochim. Acta* **57**, 1 (1992).

[36] D. Adel *et al.*, «Experimental investigation and theoretical evaluation of proton induced nuclear reactions on nickel», *Appl. Radiat. Isot.* **159**, 109094 (2020).

[37] R.A. Rebeles, P. Van den Winkel, A. Hermanne, F. Tárkányi, «New measurement and evaluation of the excitation function of ^{64}Ni(p,n) reaction for the production of ^{64}Cu», *Nucl. Instrum. Methods Phys. Res. B* **267**, 457 (2009).

[38] S.N. Ghoshal, «An Experimental Verification of the Theory of Compound Nucleus», *Phys. Rev.* **80**, 939 (1950).

[39] R. Colle, R. Kishore, J. Cumming, «Excitation functions for (p,n) reactions to 25 MeV on ^{63}Cu, ^{65}Cu, and ^{107}Ag», *Phys. Rev. C* **9**, 1819 (1974).

[40] M. Hille, P. Hille, M. Uhl, W. Weisz, «Excitation functions of (p,n) and (α,n) reactions on Ni, Cu and Zn», *Nucl. Phys. A* **198**, 625 (1972).

[41] J. Meadows, «Excitation Functions for Proton-Induced Reactions with Copper», *Phys. Rev.* **91**, 885 (1953).

[42] P. Dmitriev, I. Konstantinov, N. Krasnov, «Excitation function for the $Cu^{65}(p,n)Zn^{65}$ reaction», *Sov. At. Energy* **24**, 346 (1968).

[43] S. Kormali, D. Swindle, E. Schweikert, «Charged particle activation of medium Z elements», *J. Radioanal. Nucl. Chem.* **31**, 437 (1976).

[44] E. Gadioli *et al.*, «Excitation functions of ^{51}V, ^{56}Fe, ^{65}Cu (p,n) reactions between 10 and 45 MeV», *Nuovo Cim. A* **22**, 547 (1974).

[45] H. Howe, «(p,n) Cross Sections of Copper and Zinc», *Phys. Rev.* **109**, 2083 (1958).

[46] F. Szelecsényi *et al.*, «Evaluated cross section and thick target yield data bases of $Zn + p$ processes for practical applications», *Appl. Radiat. Isot.* **49**, 1005 (1998).

[47] F. Tárkányi, F. Szelecsényi, Z. Kovács, S. Sudár, «Excitation Functions of Proton Induced Nuclear Reactions on Enriched ^{66}Zn, ^{67}Zn and ^{68}Zn», *Radiochim. Acta* **50**, 19 (1990).

[48] A. Hermanne, «Evaluated cross section and thick target yield data of $Zn + p$ processes for practical applications», EXFOR 4093, 1997, https://www-nds.iaea.org/exfor//servlet/X4sX4arc?op=sacmp&subent=D4093008&reqx=1083

[49] F.E. Little, M.C. Lagunas-Solar, «Cyclotron production of ^{67}Ga. Cross sections and thick-target yields for the $^{67}Zn(p,n)$ and $^{68}Zn(p,2n)$ reactions», *Int. J. Appl. Radiat. Isot.* **34**, 631 (1983).

[50] S. Braccini *et al.*, «Optimization of ^{68}Ga production at an 18 MeV medical cyclotron with solid targets by means of cross-section measurement of ^{66}Ga, ^{67}Ga and ^{68}Ga», *Appl. Radiat. Isot.* **186**, 110252 (2022).

[51] H. Naik, S. Suryanarayana, M. Murali, R. Kapote Noy, «Excitation function of $^{68}Zn(p,n)^{68}Ga$ reaction for the production of ^{68}Ga», *J. Radioanal. Nucl. Chem.* **324**, 285 (2020).

[52] F. Szelecsényi *et al.*, «Investigation of direct production of ^{68}Ga with low energy multiparticle accelerator», *Radiochim. Acta* **100**, 5 (2012).

[53] N. Porile *et al.*, «Nuclear reactions of Ga^{69} and Ga^{71} with 13–56 MeV protons», *Nucl. Phys.* **43**, 500 (1963).

[54] A. Mushtaq, S. Qaim, G. Stöcklin, «Production of ^{73}Se via $(p,3n)$ and $(d,4n)$ reactions on arsenic», *Int. J. Rad. Appl. Instrum. A* **39**, 1085 (1988).

[55] J.C. Brodovitch, J.J. Hogan, K.I. Burns, «The pre-equilibrium statistical model: Comparison of calculation with two (p,xn) reactions», *J. Inorg. Nucl. Chem* **38**, 1581 (1976).

[56] H. Hassan *et al.*, «Experimental studies and nuclear model calculations on proton-induced reactions on ^{nat}Se, ^{76}Se and ^{77}Se with particular reference to the production of the medically interesting radionuclides ^{76}Br and ^{77}Br», *Appl. Radiat. Isot* **60**, 899 (2004).

[57] Z. Kovács, G. Blessing, S. Qaim, G. Stöcklin, «Production of ^{75}Br via the $^{76}Se(p,2n)^{75}Br$ reaction at a compact cyclotron», *Int. J. Appl. Radiat. Isot.* **36**, 635 (1985).

[58] H.I. West, Jr. *et al.*, «Bromine and iodine excitation-function measurements with protons and deuterons at 3–17 MeV», *Phys. Rev. C* **47**, 248 (1993).

[59] M. Dikšić, J.-L. Galinier, H. Marshall, L. Yaffe, «^{79}Br and ^{81}Br(p,xn) and $(p,pxn\ )$ excitation functions in the energy range 10–85 MeV», *Phys. Rev. C* **19**, 1753 (1979).

[60] Z. Kovács, F. Tárkányi, S. Qaim, G. Stöcklin, «Excitation functions for the formation of some radioisotopes of rubidium in proton induced nuclear reactions on $^{\rm nat}$Kr, ^{82}Kr and ^{83}Kr with special reference to the production of ^{81}Rb(^{81m}Kr) generator radionuclide», *Int. J. Rad. Appl. Instrum. A* **42**, 329 (1991).

[61] S. Kastleiner *et al.*, «Excitation functions of ^{85}Rb$(p,xn)^{85m,g,83,82,81}$Sr reactions up to 100 MeV: integral tests of cross section data, comparison of production routes of ^{83}Sr and thick target yield of ^{82}Sr», *Appl. Radiat. Isot.* **56**, 685 (2002).

[62] M.S. Uddin *et al.*, «Accurate determination of production data of the non-standard positron emitter ^{86}Y via the ^{86}Sr(p,n)-reaction», *Radiochim. Acta* **108**, 747 (2020).

[63] F. Rösch, S. Qaim, G. Stöcklin, «Nuclear Data Relevant to the Production of the Positron Emitting Radioisotope ^{86}Y via the ^{86}Sr(p,n)- and $^{\rm nat}$Rb(^{3}He,xn)-Processes», *Radiochim. Acta* **61**, 1 (1993).

[64] D. Sachdev, N. Porile, L. Yaffe, «Reactions of ^{86}Sr with protons of energies 7–85 MeV», *Can. J. Chem.* **45**, 1149 (1967).

[65] B. Satheesh, M. Musthafa, B. Singh, R. Prasad, «Nuclear Isomers ^{90,m,g}Zr, ^{89,m,g}Zr, ^{89,m,g}Y, and ^{85,m,g}Sr Formed by Bombardment of ^{89}Y with Protons of Energies from 4 to 40 MeV», *Int. J. Mod. Phys. E* **20**, 2119 (2011).

[66] H. Omara *et al.*, «Proton induced reactions on ^{89}Y with particular reference to the production of the medically interesting radionuclide ^{89}Zr», *Radiochim. Acta* **97**, 467 (2009).

[67] M.U. Khandaker *et al.*, «Investigations of ^{89}Y$(p,x)^{86,88,89g}$Zr, $^{86m+g,87g,87m,88g}$Y, ^{85g}Sr, and ^{84g}Rb nuclear processes up to 42 MeV», *Nucl. Instrum. Methods Phys. Res. B* **271**, 72 (2012).

[68] M. Mustafa *et al.*, «Measurements and a direct-reaction plus Hauser–Feshbach analysis of ^{89}Y$(p,n)^{89}$Zr, ^{89}Y$(p,2n)^{88}$Zr, and ^{89}Y$(p,pn)^{88}$Y reactions up to 40 MeV», *Phys. Rev. C* **38**, 1624 (1988).

[69] G. Saha, N. Porile, L. Yaffe, «(p,xn) and (p,pxn) Reactions of Yttrium-89 with 5–85-MeV Protons», *Phys. Rev.* **144**, 962 (1966).

[70] R. Michel *et al.*, «Cross sections for the production of residual nuclides by low- and medium-energy protons from the target elements C, N, O, Mg, Al, Si, Ca, Ti, V, Mn, Fe, Co, Ni, Cu, Sr, Y, Zr, Nb, Ba and Au», *Nucl. Instrum. Methods Phys. Res. B* **129**, 153 (1997).

[71] S. Busse, F. Rösch, S.M. Qaim, «Cross section data for the production of the positron emitting niobium isotope ^{90}Nb via the ^{90}Zr(p,n)-reaction», *Radiochim. Acta* **90**, 1 (2002).

[72] E. Lamere *et al.*, «Proton-induced reactions on molybdenum», *Phys. Rev. C* **100**, 034614 (2019).

[73] S. Sudár, F. Cserpák, S. Qaim, «Measurements and nuclear model calculations on proton-induced reactions on ^{103}Rh up to 40 MeV: evaluation of the excitation function of the ^{103}Rh$(p,n)^{103}$Pd reaction relevant to the production of the therapeutic radionuclide ^{103}Pd», *Appl. Radiat. Isot.* **56**, 821 (2002).

[74] A. Hermanne, M. Sonck, A. Fenyvesi, L. Daraban, «Study on production of ^{103}Pd and characterisation of possible contaminants in the proton irradiation of ^{103}Rh up to 28 Mev», *Nucl. Instrum. Methods Phys. Res. B* **170**, 281 (2000).

[75] P. Dmitriev, I. Konstantinov, N. Krasov, «Excitation functions of the reactions Ag$^{109}(p,n)$; Ag$^{109}(d,2n)$; Ag$^{107}(\alpha,2n+pn)$, and yield of Cd^{109}», *Sov. At. Energy* **22**, 386 (1967).

[76] E. Skakun, A. Kljucharev, Y.N. Rakivnenko, I. Romanij, «Excitation functions of (p,n) and $(p,2n)$ reactions on cadmium isotopes», *Bull. Russ. Acad. Sci.* **39**, 18 (1975).

[77] K. Otozai *et al.*, «Excitation functions for the reactions induced by protons on Cd up to 37 MeV», *Nucl. Phys.* **80**, 335 (1966).

[78] F. Tárkányi *et al.*, «Cross sections of proton induced nuclear reactions on enriched ^{111}Cd and ^{112}Cd for the production of ^{111}In for use in nuclear medicine», *Appl. Radiat. Isot.* **45**, 239 (1994).

[79] E.K. Elmaghraby, G.Y. Mohamed, M. Al-abyad, «Experimental investigation and nuclear model calculations for proton induced reactions on indium around thresholds», *Nucl. Phys. A* **984**, 112 (2019).

[80] H. Thisgaard, M. Jensen, «Production of the Auger emitter ^{119}Sb for targeted radionuclide therapy using a small PET-cyclotron», *Appl. Radiat. Isot.* **67**, 34 (2009).

[81] G. Hovhannisyan *et al.*, «Proton induced reactions on ^{114}Sn and ^{120}Sn targets at energies up to 18 MeV», *Eur. Phys. J. A* **59**, 161 (2023).

[82] S.V. Ermolaev *et al.*, «Cross sections and production yields of ^{117m}Sn and other radionuclides generated in natural and enriched antimony with protons up to 145 MeV», *Radiochim. Acta* **108**, 327 (2020).

[83] A. Hohn, H. Coenen, S. Qaim, «Nuclear data relevant to the production of ^{120g}I via the ^{120}Te(p,n)-Process at a Small-Sized Cyclotron», *Appl. Radiat. Isot.* **49**, 1493 (1998).

[84] I. Mahunka *et al.*, «Iodine-123 production at a small cyclotron for medical use», *J. Radioanal. Nucl. Chem. Lett.* **213**, 135 (1996).

[85] B. Scholten, S. Qaim, G. Stöcklin, «Excitation functions of proton induced nuclear reactions on natural tellurium and enriched ^{123}Te: Production of ^{123}I via the ^{123}Te$(p,n)^{123}$I-process at a low-energy cyclotron», *Int. J. Radiat. Appl. Instrum. A.* **40**, 127 (1989).

[86] B. Scholten, Z. Kovács, F. Tárkányi, S. Qaim, «Excitation functions of ^{124}Te$(p,xn)^{124,123}$I reactions from 6 to 31 MeV with special reference to the production of ^{124}I at a small cyclotron», *Appl. Radiat. Isot.* **46**, 255 (1995).

[87] K. Kondo, R. Lambrecht, A. Wolf, «Iodine-123 production for radiopharmaceuticals-XX: Excitation functions of the ^{124}Te$(p,2n)^{123}$I and ^{124}Te$(p,n)^{124}$I reactions and the effect of target enrichment on radionuclidic purity», *Int. J. Appl. Radiat. Isot.* **28**, 395 (1977).

[88] A. Hohn *et al.*, «Excitation functions of ^{125}Te(p,xn)-reactions from their respective thresholds up to 100 MeV with special reference to the production of ^{124}I», *Appl. Radiat. Isot.* **55**, 149 (2001).

[89] B. Scholten *et al.*, «Comparative studies on the production of the medically important radionuclide ^{124}I via p-, d-, ^{3}He- and α-particle induced reactions», *Web of Conf.* **ND 2007**, 359 (2007).

[90] A. Vasidov, G. Vakilova, S. Muhammedov, «The excitation functions of nuclear reactions (p,n) on the isotopes Te, Cs, Ba», *Izv. Akad. Nauk Uzb. SSR, Ser. Fiz.-Mat.* **3**, 93 (1981).

[91] A. Azzam *et al.*, «Excitation functions for proton-induced reactions on Te and $^{\mathrm{nat}}$Ti targets: Measurements and model calculations special relevant to the ^{128}Te$(p,n)^{128}$I reaction», *Nucl. Phys. A* **999**, 121790 (2020).

[92] M.C. Lagunas-Solar *et al.*, «Cyclotron production of high-purity ^{123}I. A revision of excitation functions, thin-target and cumulative yields for ^{127}I(p,xn) reactions», *Int. J. Radiat. Appl. Instrum. A* **37**, 823 (1986).

[93] F. Tárkányi *et al.*, «Cross section measurements of the ^{131}Xe(p,n) reaction for production of the therapeutic radionuclide ^{131}Cs», *Appl. Radiat. Isot.* **67**, 1751 (2009).

[94] F. Tárkányi *et al.*, «New measurements and evaluation of excitation functions for (p,xn), (p,pxn) and $(p,2pxn)$ reactions on ^{133}Cs up to 70 MeV proton energy», *Appl. Radiat. Isot.* **68**, 47 (2010).

[95] H.E. Hassan *et al.*, «Proton induced reactions on Tb-159 and La-139 for producing Dy and Ce-139», in: «Proceedings of the 6$^{\mathrm{th}}$ International Conference on Nuclear and Particle Physics (NUPPAC'07)», Luxor, Egypt November 17–21, 2007, p. 209.

[96] M. Furukawa, «Excitation functions for proton-induced reactions of ^{140}Ce and ^{142}Ce up to $E_p = 15$ MeV», *Nucl. Phys. A* **90**, 253 (1967).

[97] E. Verdieck, J. Miller, «Radiative Capture and Neutron Emission in La$^{139} + \alpha$ and Ce$^{142} + p$», *Phys. Rev.* **153**, 1253 (1967).

[98] M. Aikawa, Y. Hanada, H. Huang, H. Haba, «Activation cross sections of proton-induced reactions on praseodymium up to 30 MeV», *Nucl. Instrum. Methods Phys. Res. B* **508**, 29 (2021).

[99] K. Hilgers, Y.N. Shubin, H.H. Coenen, S.M. Qaim, «Experimental measurements and nuclear model calculations on the excitation functions of $^{\mathrm{nat}}$Ce(^{3}He,xn) and ^{141}Pr(p,xn) reactions with special reference to production of the therapeutic radionuclide Nd», *Radiochim. Acta* **93**, 553 (2005).

[100] D. Aumann, W. Gueckel, «Absolute cross sections and isomeric cross-section ratios for the ^{148}Nd$(d,2n)$, ^{148}Nd(p,n), and ^{146}Nd(α,pn) reactions producing the isomeric pair ^{148}Pm^{m,g}», *Phys. Rev. C* **16**, 160 (1977).

[101] D. Banerjee *et al.*, «Role of p-induced population of medium-mass $(A \sim 150)$ neutron-rich nuclei», *Phys. Rev. C* **91**, 024617 (2015).

[102] K. Katoh *et al.*, «Production of ^{147}Eu for Gamma-Ray Emission Probability Measurement», *J. Nucl. Sci. Technol.* **39**, 329 (2002).

[103] H. West *et al.*, «Proton and deuteron excitation functions for Eu-151 and Eu-153», *Brookhaven Natl. Lab. Rep.* **42382**, 87 (1989).

[104] R.K. Chapman *et al.*, «Measurement of the ^{160}Gd$(p,n)^{160}$Tb excitation function from 4–18 MeV using stacked-target activation», *Appl. Radiat. Isot.* **171**, 109647 (2021).

[105] C. Birattari *et al.*, «Pre-equilibrium processes in (p,n) reactions», *Nucl. Phys. A* **201**, 579 (1973).

[106] F. Tárkányi *et al.*, «Activation cross-sections of longer lived radioisotopes of proton induced nuclear reactions on terbium up to 65 MeV», *Appl. Radiat. Isot.* **127**, 7 (2017).

[107] F. Tárkányi *et al.*, «Experimental study of the ^{165}Ho(p,n) nuclear reaction for production of the therapeutic radioisotope ^{165}Er», *Nucl. Instrum. Methods Phys. Res. B* **266**, 3346 (2008).

[108] N. Gracheva *et al.*, «^{165}Er: A new candidate for Auger electron therapy and its possible cyclotron production from natural holmium targets», *Appl. Radiat. Isot.* **159**, 109079 (2020).

[109] G. Beyer, S. Zeisler, D. Becker, «The Auger-electron emitter ^{165}Er: excitation function of the ^{165}Ho(p,n) Er process», *Radiochim. Acta* **92**, 219 (2004).

[110] J. Červenák, K.O. Fialová, L. Ondrák, O. Lebeda, «New cross sections for ^{165}Ho(p,x) reactions focused on production of a perspective Auger electron emitter ^{165}Er», *Appl. Radiat. Isot.* **225**, 112088 (2025).

[111] F. Tárkányi *et al.*, «Experimental study of the excitation functions of proton induced nuclear reactions on ^{167}Er for production of medically relevant ^{167}Tm», *Appl. Radiat. Isot.* **68**, 250 (2010).

[112] G. Dellepiane *et al.*, «Cross-section measurement of thulium radioisotopes with an 18 MeV medical PET cyclotron for an optimized ^{165}Er production», *Appl. Radiat. Isot.* **200**, 110954 (2023).

[113] A. Hermanne *et al.*, «Cross sections for production of longer lived ^{170,168,167}Tm in 16 MeV proton irradiation of $^{\mathrm{nat}}$Er», *Nucl. Instrum. Methods Phys. Res. B* **269**, 695 (2011).

[114] I. Spahn *et al.*, «Cross-section measurement of the ^{169}Tm(p,n) reaction for the production of the therapeutic radionuclide ^{169}Yb and comparison with its reactor-based generation», *Appl. Radiat. Isot.* **63**, 235 (2005).

[115] M. Saito *et al.*, «Production cross sections of ^{169}Yb by the proton-induced reaction on ^{169}Tm», *Nucl. Instrum. Methods Phys. Res. B* **471**, 13 (2020).

[116] N.N. Krasnov, P.P. Dmitriev, «Excitation functions and yields of the reactions ^{181}Ta$(d, 2n)^{181}$W and ^{181}Ta$(p, n)^{181}$W», *Sov. At. Energy* **20**, 189 (1966).

[117] B. Ali, G.Y. Mohamed, M. Al-Abyad, «Activation cross sections of proton induced nuclear reactions on tungsten: Special regard to the formation of ^{186}Re», *Nucl. Phys. A* **1045**, 122833 (2024).

[118] S. Lapi *et al.*, «Production cross-sections of $^{181-186}$Re isotopes from proton bombardment of natural tungsten», *Appl. Radiat. Isot.* **65**, 345 (2007).

[119] F. Tárkányi *et al.*, «Upgrade of recommended nuclear cross section data base for production of therapeutic radionuclides», *J. Radioanal. Nucl. Chem.* **331**, 1163 (2022).

[120] F. Szelecsényi *et al.*, «Study of production possibility of no-carrier-added ^{186}Re via proton induced reactions on tungsten», in: «Proceedings of the Sixth International Symposium on Synthesis, Applications of Isotopically Labelled Compounds», *John Wiley & Sons*, Philadelphia, PA, USA September 14–18, 1997, p. 701.

[121] F. Szelecsényi *et al.*, «Excitation functions of ^{186,187,188,189,190,192}Ir formed in proton-induced reactions on highly enriched ^{192}Os up to 66 MeV», *Nucl. Instrum. Methods Phys. Res. B* **268**, 3306 (2010).

[122] M. Hemalatha *et al.*, «Evolution of (p, n) reaction cross sections for Au isotopes», in: «Proceedings of the DAE Symp. on Nucl. Phys.», Volume 69, 2025, p. 639.

[123] L.F. Hansen, R.D. Albert, «Statistical Theory Predictions for 5- to 11-MeV (p, n) and (p, p') Nuclear Reactions in V51, Co^{59}, Cu^{63}, Cu^{65}, and Rh^{103}», *Phys. Rev.* **128**, 291 (1962).

[124] J. Červenák, O. Lebeda, «Measurement of cross-sections of proton-induced nuclear reactions on ^{197}Au focused on the production of the theranostic pair ^{197m,g}Hg», *Nucl. Instrum. Methods Phys. Res. B* **458**, 118 (2019).

[125] E. Elmaghraby, K. Hassan, H. Omara, Z. Saleh, «Production of the mercury-197 through proton induced reaction on gold», *Appl. Radiat. Isot.* **68**, 1694 (2010).

[126] B. Satheesh, M. Musthafa, B. Singh, R. Prasad, «Study of Isomeric Cross-Section Ratio and Pre-Equilibrium Fraction in Proton and Alpha Particle Induced Nuclear Reactions on ^{197}Au», *Int. J. Mod. Phys. E* **21**, 1250059 (2012).

[127] T. Kotanjyan *et al.*, «Electronic properties of ionizing radiation-induced defects at SiO_2/Si interface associated with non-trivial excess current splitting», *Eur. Phys. J. Plus* **139**, 1 (2024).

[128] R. Bell, H. Skarsgard, «Cross Sections of (p, xn) Reactions in the Isotope of Lead and Bismuth», *Can. J. Phys.* **34**, 745 (1956).

[129] K. Miyano *et al.*, «The (p, n) Reaction on ^{209}Bi and Pre-Compound Process», *J. Phys. Soc. Jpn.* **45**, 1071 (1978).